CuO_6 octahedron[20] as well as the enhancement due to increased magnetic dipole transition probability. The latter observation supports our contention that the metal ions are exchange coupled.

Acknowledgments. S.H.W. thanks Dr. George A. Candela of the National Bureau of Standards for lending his expertise in the magnetic susceptibility measurements, A.L.R. thanks NSF for supporting the purchase of the diffractometer, and G.F.K. acknowledges the donors of the Petroleum Research Fund, administered by the American Chemical Society, for partial support of this work.

Registry No. $Na_{10}[Fe_4Cu_2W_{18}O_{70}H_6]\cdot 29H_2O$, 109466-62-8; $Fe(NO_3)_3$, 10421-48-4; $Cu(CH_3COO)_2$, 142-71-2; Na_2WO_4, 13472-45-2.

Supplementary Material Available: Tables 2S–4S, listing bond distances and angles and anisotropic thermal parameters (7 pages); Table 1S, listing observed and calculated structure factors (29 pages). Ordering information is given on any current masthead page.

Contribution from the Laboratoire de Spectrochimie des Elêments de Transition, UA No. 420, Université de Paris-Sud, 91405 Orsay, France, and Departament de Cristal.lografia i Mineralogia, Universitat de Barcelona, 08007 Barcelona, Spain

Magnetic Interaction and Spin Transition in Iron(II) Dinuclear Compounds. Crystal Structure of (μ-2,2′-Bipyrimidine)bis[(2,2′-bipyrimidine)bis(thiocyanato)iron(II)]

Antonio Real,[1a,c] Jacqueline Zarembowitch,[1a] Olivier Kahn,*[1a] and Xavier Solans[1b]

Received March 13, 1987

Three iron(II) dinuclear compounds of general formula $[FeL(NCS)_2]_2$bpym have been synthesized. Bpym is the bridging ligand 2,2′-bipyrimidine. L is bpym (**1**), bpy (2,2′-bipyridine; **2**), or bzp (bromazepan; **3**). The crystal structure of **1** has been solved. **1** crystallizes in the triclinic system, space group $P\bar{1}$, with a = 11.622 (3) Å, b = 9.138 (2) Å, c = 9.241 (2) Å, α = 118.74 (2)°, β = 74.39 (2)°, γ = 99.85 (2)°, and Z = 1. The structure consists of centrosymmetric dinuclear units with two NCS groups in a cis position, a terminal bpym, and two nitrogen donors of the bridging bpym around each iron. The magnetic properties of **1–3** have been investigated down to 4.2 K. In **1** and **2**, the iron(II) ions are high spin in the whole temperature range and interact in an antiferromagnetic fashion with J = −4.1 cm^{-1} in **1** and −4.9 cm^{-1} in **2** ($\mathcal{H} = -J\hat{S}_A\cdot\hat{S}_B$). In **3**, a gradual and incomplete spin transition occurs around 235 K. Below the transition, the compound consists of roughly 52% of the diamagnetic SS species, 40% of the antiferromagnetically coupled QQ species, and only 8% of the electronically dissymmetric SQ species (S = local singlet, Q = local quintet).

Introduction

The first report by Cambi on a metal complex exhibiting a temperature-induced low-spin ↔ high-spin transition appeared more than half a century ago.[2] Nevertheless, this field remains very active,[3,4] and great strides have been made in the last few years. The mechanism of the phenomenon is today reasonably well understood, at least qualitatively.[4,5] In particular, it has been conclusively pointed out that the abruptness of the transition is related to the cooperativity of the phenomenon within the crystal lattice.[6] Slichter and Drickamer have proposed a thermodynamic approach to an understanding of the spin transition in which this cooperativity is accounted for by an interaction Gibbs free energy.[6,7] This approach, similar to that utilized for the regular solutions, may fairly well reproduce the more or less abrupt nature of the transition, as well as the eventual hysteresis effect.[4,8,9] Another recent break-through in this area is the discovery of the LIESST (light-induced excited-spin-state trapping) phenomenon; Decurtins et al. have shown that it was possible to convert optically the low-spin phase into the high-spin phase in the very low temperature range where the low-spin phase is thermodynamically stable.[10,11]

The renewed interest brought to spin transitions is due, among other reasons, to the fact that this phenomenon is one of the most spectacular examples of bistability in inorganic chemistry. The spin transition may be very abrupt—the total conversion may occur within less than 1 K—and may exhibit an hysteresis. It follows that a spin transition system could potentially be utilized as an element of a molecular device able to store information. In other words, if we consider the low-spin/high-spin transformation

$$\underset{1-x}{\text{LS}} \leftrightarrow \underset{x}{\text{HS}} \qquad (1)$$

which is assumed to be abrupt, where x is the molar fraction of high-spin form at a given temperature, the x vs. T plot (or the $\chi_M T$ vs. T plot, χ_M being the molar magnetic susceptibility) schematized in Figure 1 may be seen as a signal, in the general sense of the term.

A difficulty, however, arises along this line. For a mononuclear spin transition compound, the low-spin phase is always the stable phase below the critical temperature T_c. This situation may be understood on the basis of very simple thermodynamical considerations. At the temperature T_c, we have

$$\Delta G = \Delta H - T_c\Delta S = 0 \qquad (2)$$

where the variations of Gibbs free energy $\Delta G = G_{HS} - G_{LS}$, of enthalpy $\Delta H = H_{HS} - H_{LS}$ and of entropy $\Delta S = S_{HS} - S_{LS}$ refer to the transformation (1). ΔS is positive. Indeed, the electronic degeneracy and hence the electronic entropy are higher in the HS phase than in the LS phase. Moreover, in the HS phase, the metal–ligand bond lengths are, on average, longer, so that the internal vibrational entropy, which is the main component of the total vibrational entropy,[3] is also higher in this phase than in the LS phase. Since ΔS is positive, from (2) ΔH is positive too. Below T_c, ΔG is positive and the LS phase is stable; above T_c, the reverse situation holds. To sum up this point, we can say that with a mononuclear compound exhibiting a spin transition, the most likely type of signal is that schematized in Figure 1; above T_c, we have a strong response and below T_c, a weak response. An exception would be possible with a compound presenting either two spin

(1) (a) Université de Paris-Sud. (b) Universitat de Barcelona. (c) On leave from the Department of Inorganic Chemistry, University of Valencia, Spain.
(2) Cambi, L.; Cagnasso, A. *Atti Accad. Naz: Lincei, Cl. Sci. Fis. Mat. Nat., Rend.* **1931**, *13*, 809.
(3) Gütlich, P. *Struct. Bonding (Berlin)* **1981**, *44*, 83.
(4) König, E.; Ritter, G.; Kulshreshtha, S. K. *Chem. Rev.* **1985**, *85*, 219.
(5) Rao, C. N. R. *Internat. Rev. Phys. Chem.* **1985**, *4*, 19.
(6) Slichter, C. P.; Drickamer, H. G. *J. Chem. Phys.* **1972**, *56*, 2142.
(7) Drickamer, H. G.; Frank, C. W. *Electronic Transitions and the High Pressure Chemistry and Physics of Solids*; Chapman and Hall: London, 1973.
(8) Zarembowith, J.; Claude, R.; Kahn, O. *Inorg. Chem.* **1985**, *24*, 1576.
(9) Purcell, K. F.; Edwards, M. P. *Inorg. Chem.* **1984**, *23*, 2620.
(10) Decurtins, S.; Gütlich, P.; Köhler, C. P.; Spiering, H.; Hauser, A. *Chem. Phys. Lett.* **1984**, *105*, 1.
(11) Decurtins, S.; Gütlich, P.; Hasselbach, K. M.; Hauser, A.; Spiering, H. *Inorg. Chem.* **1985**, *24*, 2174.

0020-1669/87/1326-2939$01.50/0

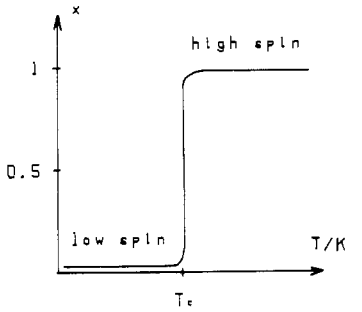

Figure 1. x vs. T plot for a low-spin/high-spin transformation in a mononuclear species. x is the molar fraction of high-spin species.

transitions $S = 0 \leftrightarrow S = 1$ and $S = 1 \leftrightarrow S = 2$ for an iron(II) compound, with well-separated critical temperatures, or a unique transition, without intermediate spin, but occurring in two steps. To our knowledge, there is no report on compounds of the former kind. On the other hand, two-step transitions have already been observed.[12-14]

With homo- or heteropolymetallic systems in which spin transition and exchange interaction coexist, it appears conceivable to obtain novel kinds of $\chi_M T$ vs. T plots, i.e. novel kinds of signals. That is why we have decided to explore this rather novel field. Our ultimate goal is to utilize the spin transition phenomenon for signal processing, and this paper is the first one dealing with this idea. To our knowledge, five studies devoted to polymetallic systems exhibiting a spin transition have already been published. One of them concerns iron(III) dinuclear species,[15] two of them concern linear trinuclear species in which only the central metal ion, Co(III)[16,17] or Fe(III),[18] undergoes the spin transition, the fourth study deals with an iron(II) two-dimensional compound,[19] and the last one deals with the cluster compound Nb_6I_{11}.[20]

In the first four cases, the metal centers are apparently too far apart to interact significantly. In contrast, in Nb_6I_{11}, the niobium atoms are strongly bonded. It turns out that none of these polymetallic compounds is appropriate to investigate the eventual synergistic effect of the exchange interaction and the spin transition.

In this paper, we report on the iron(II) dinuclear compounds of general formula $[FeL(NCS)_2]_2$bpym. Bpym is the bis bidentate bridging ligand 2,2′-bipyrimidine. L is the bidentate terminal ligand bpym (**1**), bpy (2,2′-bipyridine; **2**) or bzp (bromazepan; (**3**).

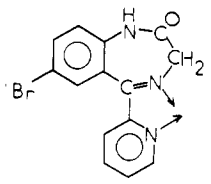

3

Experimental Section

Syntheses. $Fe(py)_4(NCS)_2$ (py = pyridine) was obtained according to the described procedure.[21]

Table I. Conditions for Crystallographic Data Collection and Structure Refinement of **1**

formula	$C_{28}H_{18}N_{16}S_4Fe_2$
fw	818.5
cryst syst	triclinic
a, Å	11.622 (3)
b, Å	9.138 (2)
c, Å	9.241 (2)
α, deg	118.74 (2)
β, deg	74.39 (2)
γ, deg	99.85 (2)
V, Å^3	827.8 (6)
space group	$P\bar{1}$
D_{calcd}, g cm^{-3}	1.641
Z	1
$F(000)$	414
λ(Mo Kα), Å	0.710 69
μ(Mo Kα), cm^{-1}	11.93
T, K	288
diffractometer	Philips PW-1100
unit cell	25 reflcns ($4 \leq \theta \leq 12°$)
scan type	ω
scan width, deg	0.8
scan speed, deg s^{-1}	0.03
no. of measd reflcns	2123
θ range, deg	2–25
no. of obsd reflcns	1962 ($I \geq 2.5\sigma(I)$)
determination	MULTAN84
refinement	SHELX76
minimized function	$\sum w\|\|F_o\| - \|F_c\|^2\|$
weighting scheme	$(\sigma^2(F_o) + 0.0006\|F_o\|^2)^{-1}$
final R	0.059
R_w	0.064
max peak in final $\Delta\rho$, e Å^{-3}	0.2
max shift/esd	0.14

$[Fe(bpym)(NCS)_2]_2$bpym (**1**) was synthesized as follows: 20 mL of a methanolic solution containing 1 mmol of bpym was added to 40 mL of a methanolic solution containing 0.67 mmol of $Fepy_4(NCS)_2$, at 60 °C and under argon. **1** precipitated as a dark violet microcrystalline powder, was washed with methanol and dried under vacuum. Single crystals of **1** were obtained by slow diffusion of the methanolic solutions in an H-shaped tube over 3 or 4 weeks.

Anal. Calcd for $C_{28}H_{19}N_{16}O_{0.5}S_4Fe_2$ (**1**·0.5H_2O): C, 40.64; H, 2.31; N, 27.08; S, 15.50; Fe, 13.49. Found: C, 40.64; H, 2.46; N, 26.85; S, 15.52; Fe, 13.30.

$[Fe(bpy)(NCS)_2]_2$bpym (**2**) and $[Fe(bzp)(NCS)_2]_2$bpym (**3**) were synthesized as follows: 20 mL of a methanolic solution containing 1 mmol of bpy for **2**, or bzp for **3** was added to 40 mL of a methanolic solution containing 1 mmol of $Fepy_4(NCS)_2$. Then 20 mL of a methanolic solution containing 0.5 mmol of bpym was added, and the mixture was heated at reflux for 2 h. **2** or **3** precipitated as a violet microcrystalline powder, was washed with methanol, and dried under vacuum. From IR and X-ray data, we carefully checked that the compounds were not mixtures of $FeL_2(NCS)_2$ (L = bpy or bzp) and **1**. The infrared spectroscopy provides a good test to recognize a compound with a terminal bpym. The spectrum then exhibits a sharp and characteristic band at 1565 cm^{-1}, which does not exist when bpym is only bridging. This band is present in **1** but not in **2** and **3**. On the other hand, when phen = 1,10-phenanthroline is used instead of bpy or bzp, the same procedure gives a mixture of $Fe(phen)_2(NCS)_2$ and **1** and not the expected dinuclear compound.

Anal. Calcd for $C_{32}H_{26}N_{12}O_2S_4Fe_2$ (**2**·H_2O): C, 45.18; H, 3.08; N, 19.76; S, 15.07; Fe, 13.13. Found: C, 45.47; H, 3.04; N, 20.18; S, 15.09; Fe, 12.90. Calcd for $C_{40}H_{28}N_{14}O_3Br_2S_4Fe_2$ (**3**·H_2O): C, 41.68; H, 2.45; N, 17.01; S, 11.13; Fe, 9.69. Found: C, 41.97; H, 2.48; N, 16.47; S, 10.70; Fe, 9.31.

Crystallographic Data Collections and Refinement of the Structure. A prismatic crystal (0.1 × 0.1 × 0.15 mm) of **1** was selected and mounted on a Philips PW-1100 four-circle diffractometer. Information concerning conditions for crystallographic data collection and structure refinement is summarized in Table I. Unit-cell parameters were determined from 25 reflections and refined by a least-squares method. A total of 2123 reflections were measured in the range $2° \leq \theta \leq 25°$; 1962 of them were assumed as observed from the condition $I \geq 2.5\sigma(I)$. Three reflections were measured every 2 h as an orientation and intensity control, and no significant intensity decay was observed. A Lorentz-polarization correction was made, but no absorption corrections were made. The structure was solved by direct methods using the MULTAN84 system of computer programs[22] and refined by full-matrix least squares using the

(12) Köppen, H.; Müller, E. W.; Köhler, C. P.; Spiering, H.; Meissner, E.; Gütlich, P. *Chem. Phys. Lett.* **1982**, *91*, 348.
(13) Wiehl, L.; Kiel, G.; Köhler, C. P.; Spiering, H.; Gütlich, P. *Inorg. Chem.* **1986**, *25*, 1565.
(14) Petrouleas, V.; Tuchagues, J. P. *Chem. Phys. Lett.*, in press.
(15) Ohta, S.; Yoshimura, C.; Matsumoto, N.; Okawa, H.; Ohyoshi, A. *Bull. Chem. Soc. Jpn.* **1986**, *59*, 155.
(16) Eberspach, W.; El Murr, N.; Kläui, W. *Angew. Chem., Int. Ed. Engl.* **1982**, *21*, 915.
(17) Navon, G.; Kläui, W. *Inorg. Chem.* **1984**, *23*, 2722.
(18) Vos, G.; De Graaff, R. A. G.; Haasnoot, J. G.; Van Der Kraan, A. M.; de Val, P.; Reedijk, J. *Inorg. Chem.* **1984**, *23*, 2305.
(19) Vreugdenhil, W.; Gorter, S.; Haasnoot, J. G.; Reedijk, J. *Polyhedron* **1985**, *4*, 1769.
(20) Imoto, H.; Simon, A. *Inorg. chem.* **1982**, *21*, 308.
(21) Grossmann, H.; Hünseller, F. *Z. Anorg. Allg. Chem.* **1905**, *46*, 370.

Table II. Atomic Coordinates ($\times 10^4$) for the Non-Hydrogen Atoms in **1**

	x/a	y/b	z/c	B_{eq}[a] Å^2
Fe	7966 (1)	2119 (1)	7603 (2)	4.0 (6)
N1	8834 (6)	4323 (9)	7652 (10)	5.16 (39)
C1	9004 (6)	5540 (10)	7491 (11)	4.26 (41)
S1	9276 (2)	7204 (3)	7220 (3)	5.61 (13)
N2	6427 (6)	2550 (9)	7216 (10)	5.43 (41)
C2	5539 (7)	2928 (11)	7185 (12)	4.90 (46)
S2	4303 (2)	3511 (3)	7169 (4)	6.25 (15)
N3	6993 (5)	93 (8)	8149 (9)	4.10 (33)
C4	6498 (7)	−1320 (10)	7050 (12)	4.48 (43)
C5	5891 (7)	−2513 (11)	7547 (13)	5.23 (49)
C6	5822 (8)	−2197 (12)	9170 (14)	5.45 (52)
N7	6259 (6)	−779 (9)	10330 (9)	4.95 (38)
C8	6813 (6)	313 (10)	9725 (11)	4.12 (40)
C9	7257 (6)	1970 (10)	10989 (11)	4.20 (41)
N10	7126 (6)	2280 (9)	12582 (10)	5.18 (40)
C11	7575 (9)	3761 (13)	13604 (13)	5.72 (54)
C12	8091 (7)	4946 (12)	13087 (13)	5.22 (49)
C13	8187 (7)	4534 (11)	11430 (13)	5.00 (48)
N14	7773 (5)	3034 (8)	10345 (8)	3.66 (30)
C15	10327 (6)	229 (10)	5686 (11)	3.66 (39)
N16	9779 (5)	1134 (8)	7261 (9)	3.90 (33)
C17	10390 (7)	1532 (10)	8472 (11)	3.89 (39)
C18	11541 (8)	993 (12)	8013 (14)	4.81 (50)
C19	12038 (7)	60 (12)	6351 (13)	4.34 (45)
N20	11427 (5)	−376 (7)	5120 (8)	3.52 (29)

[a] Values for anisotropically refined atoms are given in the form of the isotropic equivalent thermal parameter $B_{eq} = (8\pi^2/3)\sum_i\sum_j U_{ij}a_i^*a_j^*a_ia_j$.

Table III. Bond Lengths (Å) in **1**

Fe–N1	2.078 (6)	C8–N3	1.332 (10)
Fe–N2	2.051 (7)	C8–C9	1.510 (11)
Fe–N3	2.200 (6)	C9–N10	1.327 (10)
Fe–N14	2.211 (6)	N10–C11	1.338 (11)
Fe–N16	2.316 (6)	C11–C12	1.371 (12)
Fe–N20	2.223 (6)	C12–C13	1.367 (12)
N1–C1	1.168 (9)	C13–N14	1.352 (10)
C1–S1	1.623 (8)	N14–C9	1.351 (9)
N2–C2	1.158 (10)	C15–N16	1.316 (10)
C2–S2	1.616 (8)	C15–N20	1.349 (9)
N3–C4	1.352 (9)	C15–C15*	1.502 (14)
C4–C5	1.393 (11)	N16–C17	1.355 (9)
C5–C6	1.366 (13)	C17–C18	1.390 (11)
C6–N7	1.349 (11)	C18–C19	1.361 (13)
N7–C8	1.358 (9)	C19–N20	1.363 (9)
		Fe–Fe	5.522 (6)

Table IV. Selected Bond Angles (deg) in **1**

N1–Fe–N2	93.5 (3)	N16–Fe–N20	72.1 (2)
N1–Fe–N3	167.6 (3)	N1–C1–Fe	158.2 (6)
N1–Fe–N14	93.5 (3)	N2–C2–Fe	172.2 (8)
N1–Fe–N16	90.1 (2)	N1–C1–S1	178.2 (8)
N1–Fe–N20	99.7 (3)	N2–C2–S2	179.0 (9)
N2–Fe–N3	89.0 (2)	Fe–N3–C8	117.4 (5)
N2–Fe–N14	108.5 (3)	N3–C8–C9	116.5 (6)
N2–Fe–N16	164.3 (3)	C8–C9–N14	114.3 (7)
N2–Fe–N20	92.2 (2)	C9–N14–Fe	117.5 (5)
N3–Fe–N14	74.2 (2)	Fe–N16–C15	115.4 (4)
N3–Fe–N16	90.7 (2)	N16–C15–C15*	118.1 (6)
N3–Fe–N20	92.3 (2)	C15*–C15–N20	114.2 (6)
N14–Fe–N16	86.5 (2)	C15–N20–Fe	119.5 (5)
N14–Fe–N20	154.7 (5)		

SHELX76 program.[23] All hydrogen atoms were located from a difference synthesis and refined with an overall isotropic temperature factor. The other atoms were refined anisotropically. The final R value was 0.059. The atomic parameters for the non-hydrogen atoms are given in Tables II and S2 (supplementary material); those for the hydrogen atoms are given in Table S1. The main bond lengths and angles are given in Tables III and IV, respectively.

(22) Main, P.; Fiske, S. E.; Hull, S. L.; Lessinger, L.; Germain, G.; Declercq, J. P.; Woolfson, M. M. "MULTAN84", University of York, England and University of Louvain, Belgium, 1984.
(23) Sheldrick, G. M. "SHELX76", University of Cambridge, England, 1976.

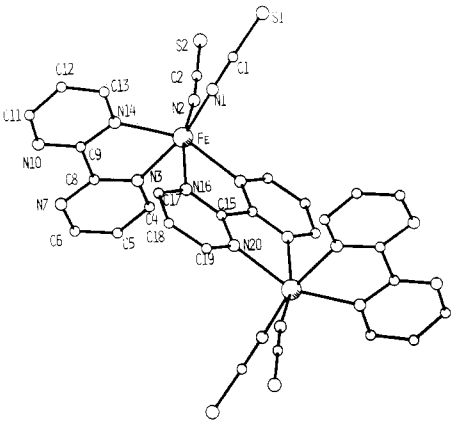

Figure 2. Perspective view of $[Fe(bpym)(NCS)_2]_2bpym$ (**1**).

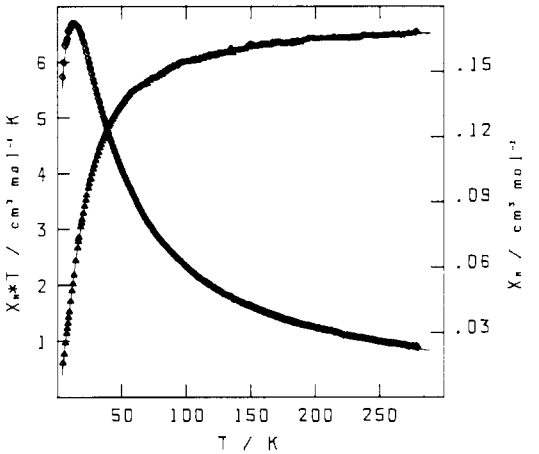

Figure 3. Experimental temperature dependence of χ_M (◇) and $\chi_M T$ (△) for **1**. Solid lines are calculated curves.

Magnetic Measurements. These were performed on powder samples, with a Faraday-type magnetometer equipped with a helium continuous-flow cryostat. Independence of the magnetic susceptibility vs. the magnetic field was checked at room temperature. $HgCo(SCN)_4$ was used as a susceptibility standard. Diamagnetic corrections were estimated at -438×10^{-6} cm^3 mol^{-1} for **1**, -394×10^{-6} cm^3 mol^{-1} for **2**, and -536×10^{-6} cm^3 mol^{-1} for **3**.

Structure of $[Fe(bpym)(NCS)_2]_2bpym$ (1)

The structure of **1** consists of centrosymmetric discrete dinuclear molecules, in which two iron(II) ions are bridged by a bpym ligand in a bis bidentate fashion. The Fe···Fe intramolecular separation is 5.522 (6) Å. A perspective view of the molecule with the labeling of the atoms is shown in Figure 2. Each iron atom is bound to six nitrogen atoms belonging to two NCS^- groups in a cis position and two bpym ligands, one being terminal, the other being bridging. The Fe–N bond lengths involving NCS^- (2.051 (7) and 2.078 (6) Å) are much shorter than those involving the bpym ligands (from 2.200 (6) to 2.316 (6) Å). Within the bridging network, Fe–N16 is significantly longer than Fe–N20 (2.316 (6) and 2.223 (6) Å, respectively). Whereas the N–C–S groups are quasi-linear, the Fe–N–C(S) linkages are significantly bent (Fe–N1–Cl) = 158.2 (6)° and Fe–N2–C2 = 172.2 (8)°). The two five-membered rings around the metal are not planar; the iron atom is out of the N3C8C9N14 and N16C15C15*N20 mean planes by 0.115 (6) and 0.269 (6) Å, respectively. The shortest intermolecular Fe···Fe separation is equal to 9.138 (2) Å.

Magnetic Properties

The magnetic properties of **1** are shown in Figure 3 in the form of both the χ_M vs. T and the $\chi_M T$ vs. T plots; χ_M is the molar magnetic susceptibility and T is the temperature. The former curve exhibits a rounded maximum at about 12 K and the latter a continuous decrease upon cooling down, with $\chi_M T = 6.53$ cm^3

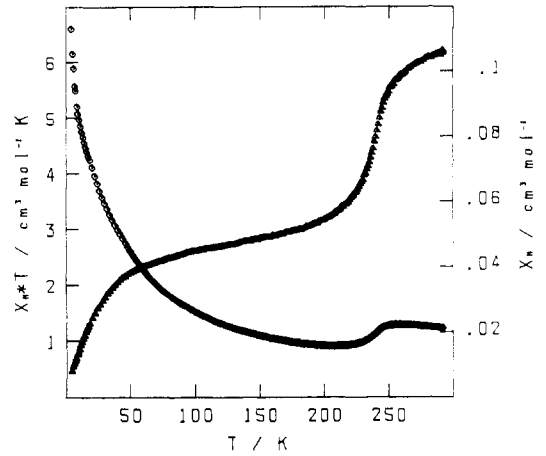

Figure 4. Experimental temperature dependence of χ_M (△) and $\chi_M T$ (◇) for **3**.

mol^{-1} K at 280 K and an extrapolated value very close to zero when T approaches zero. This behavior is characteristic of an intramolecular antiferromagnetic interaction between two high-spin iron(II) ions, with a molecular spin singlet ground state. In other words, the iron(II) ions in this compound do not present any spin transition. To interpret quantitatively the magnetic data, we used the expression for the magnetic susceptibility $\chi_M{}^D$ for a pair of local spin quintets, deduced from the spin Hamiltonian

$$\mathcal{H} = -J\hat{S}_A\cdot\hat{S}_B + g\beta(\hat{S}_A + \hat{S}_B)\cdot\vec{H} \qquad (3)$$

This expression is

$$\chi_M{}^D = \frac{2N\beta^2g^2}{kT}[\exp(J/kT) + 5\exp(3J/kT) + 14\exp(6J/kT) + 30\exp(10J/kT)]/[1 + 3\exp(J/kT) + 5\exp(3J/kT) + 7\exp(6J/kT) + 9\exp(10J/kT)] \qquad (4)$$

in which the symbols have their usual meaning. J and g were determined by minimizing $R = \sum(\chi_M{}^{obsd} - \chi_M{}^{calcd})^2/\sum(\chi_M{}^{obsd})^2$ and found as $J = -4.1$ cm^{-1} and $g = 2.13$. $R = 4.6 \times 10^{-5}$, which actually corresponds to an excellent experiment–theory agreement. We also attempted to introduce the local anisotropy of the iron(II) ion in the calculation of $\chi_M{}^D$. This anisotropy splits the excited states in the zero field. We did not get any improvement of the fitting, which suggests that the zero-field splitting of the excited states is small with regard to J.

The magnetic behavior of **2** is very similar to that of **1**. Again, the iron(II) ions are high spin in the whole temperature range and antiferromagnetically coupled within the dinuclear unit. The fitting of the magnetic data leads to $J = -4.9$ cm^{-1} and $g = 2.11$.

On the other hand, the magnetic properties of **3** reveal quite a peculiar situation. The χ_M and $\chi_M T$ vs. T plots are shown in Figure 4. χ_M first increases upon cooling from 290 down to 258 K, then decreases down to 210 K, and finally increases again, but slower than expected for the Curie law. As for $\chi_M T$, it is equal to 6.21 cm^3 mol^{-1} K at 290 K, falls down rather rapidly between 260 and 210 K and then more smoothly between 210 and 60 K, and finally falls down again rapidly below 60 K. The extrapolated value of $\chi_M T$ at 0 K is about 0.20 (3) cm^3 mol^{-1} K. This behavior may be interpretated in the following way. At room temperature, the iron(II) ions are high spin. A partial and rather smooth spin transition occurs between 260 and 220 K. Below the temperature of this incomplete transition, three kinds of dinuclear species are expected to be present: the diamagnetic SS species, the antiferromagnetically coupled QQ species similar to **1** and **2**, and the electronically dissymmetric SQ species, S stands for local singlet and Q for local quintet. The molar proportions of SS, QQ, and SQ are denoted as ρ_{SS}, ρ_{QQ}, and ρ_{SQ}, respectively. In the low-temperature range, e.g. below 150 K, the magnetic susceptibility may be expressed as

$$\chi_M = \chi_M{}^D\rho_{QQ} + \frac{2N\beta^2g^2}{kT}\rho_{SQ} \qquad (5)$$

with $\chi_M{}^D$ defined as in (4). In (5), the magnetic susceptibility of SQ is assumed to follow the Curie law. The g factor in (5) is taken equal to 2.12, the average value found for **1** and **2**. The fitting of the data leads to $\rho_{QQ} = 0.40$, $\rho_{SQ} = 0.08$, and $J = -4.9$ cm^{-1} in the QQ species, which is quite a reasonable value, close to that obtained for **1** and **2**. The R factor is then equal to 5.6×10^{-5}.

To sum up the situation encountered in **3**, we can say that at 300 K, all the dinuclear units are in a state where the two iron(II) ions are high spin. About 60% of them are involved in the smooth transition occurring around 235 K. This transition essentially gives diamagnetic dinuclear units (52%) but also a small amount of dinuclear units with a high-spin ion and a low-spin ion (8%). About 40% of the dinuclear units do not undergo the transition and, in the whole temperature range, behave as antiferromagnetically coupled species.

We reinvestigated the magnetic behavior of **3** in the temperature range where the transition happens, by cooling down and warming up successively, and we did not detect any hysteresis effect.

Discussion

There are already several reports of bpym serving as a bridging ligand in dinuclear compounds,[24-29] but the crystal structure has been solved only in the case of $[Co(hfa)_2]_2$bpym with hfa = hexafluoroacetylacetonato.[29] In this centrosymmetric compound, the two independent metal–nitrogen bond lengths involving the bridge (2.150 (3) and 2.160 (3) Å) are shorter and much closer to each other than those in **1** (2.223 (6) and 2.316 (6) Å). Surprisingly, there is also only one crystal structure of an iron(II) compound with the $FeL_2(NCS)_2$ unit, L being a bidentate ligand and the NCS groups being in a cis position.[30] This structure, of $Fe(bpy)_2(NCS)_2$, is of poor accuracy.

Several investigations dealing with the magnetic properties of 2,2′-bipyrimidine-bridged homodinuclear compounds have recently been published.[27-29] The interaction parameter J (using the interaction Hamiltonian given in (3)) was found to be on the order of -0.2 cm^{-1} for Mn(II), -1.8 cm^{-1} for Co(II), and -3 cm^{-1} for Ni(II) and in the range -4 to -90 cm^{-1} for Cu(II). In all cases, the interaction is antiferrogmagnetic. It has already been pointed out that the bis bidentate ligands leading to the bridging networks

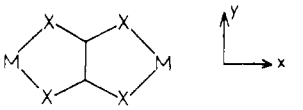

have a specific ability to favor an antiferromagnetic interaction between metal centers, provided that a magnetic orbital of xy symmetry is available on each interacting ion.[31] Such an xy-exchange pathway is operative with iron(II). Bpym is however much less efficient than the oxalato-type bridges in this respect.

Neither **1** nor **2** exhibits a spin transition. This result is rather unexpected, especialy for **2** where the environment of each iron(II) ion is chemically very close to that encountered in $Fe(bpy)_2(NCS)_2$, which undergoes an abrupt spin transition at 215 K. This behavior could be attributed to the fact that the bridging bpym exerts a weaker field than bpy. One of the structure data substantiates this hypothesis; the Fe–N16 bond length in **1**, involving the bridge (2.316 (6) Å) is significantly larger than all the Fe–N(bpy) bond lengths in $Fe(bpy)_2(NCS)_2$ (about 2.17 Å). Another possible interpretation is that the intramolecular interaction intrinsically stabilizes the high-spin state.

The most interesting compound is actually **3**, where both exchange interaction and spin transition are operative. Unfortunately, we have not been able to grow single crystals of **3** suitable

(24) Lonxa, S. *Inorg. Chim. Acta* **1983**, *75*, 131.
(25) Hunziker, M.; Ludi, A. *J. Am. Chem. Soc.* **1977**, *99*, 7370.
(26) Dose, E. V.; Wilson, L. J. *Inorg. Chem.* **1978**, *17*, 2660.
(27) Petty, R. H.; Welch, B. R.; Wilson, L. J.; Bottomley, L. A.; Kadish, K. M. *J. Am. Chem. Soc.* **1980**, *102*, 611.
(28) Overton, C.; Connor, J. A. *Polyhedron* **1982**, *1*, 53.
(29) Brewer, G.; Sinn, E. *Inorg. Chem.* **1985**, *24*, 4580.
(30) König, E.; Watson, K. J. *Chem. Phys. Lett.* **1970**, *6*, 457.
(31) Kahn, O. *Angew. Chem., Int. Ed. Engl.* **1985**, *24*, 834.

for X-ray work. To date, only one crystal structure of a metal complex with bzp has been reported.[32] This compound contains the $[(Cu(bzp))_2C_2O_4]^{2+}$ cation, and bzp is bound to copper(II) through the nitrogen atoms of both the pyridine ring and the imine group. It has already been reported that bzp can induce a spin transition in iron(II) chemistry; indeed, $Fe(bzp)_2(NCS)_2$ presents such a transition around 235 K.[33] In **3**, the transition occurs at much the same temperature, but is more gradual and very incomplete since only 56% of the metal centers become low-spin upon cooling down. Another striking aspect of the phenomenon is that, below the transition temperature, the relative proportions of SS, QQ, and SQ species do not correspond at all to the statistical proportions. If 56% of the low-spin and 44% of the high-spin iron(II) were statistically distributed among the SS, QQ, and SQ species, we would have 31.4% of SS (instead of 52%), 19.4% of QQ (instead of 40%) and 49.3% of SQ (instead of 8%). In fact, when an iron(II) ion undergoes the transition within a dinuclear unit, the other iron(II) ion of the same unit has a very high probability of undergoing the transition too, so that the formation of SQ species is unlikely. In a certain sense, the dinuclear unit itself plays the role of a small domain in which the two metal ions have the same spin state.

To conclude, we may attempt to sum up the results emerging from this study: (i) The high-spin state in the dinuclear species seems to l e stabilized with respect to what happens with mononuclear species in which the iron(II) ion has much the same environment; (ii) the spin transition, when occurring, is apparently more gradual and very incomplete in the low-temperature range; (iii) the intramolecular interaction gives rise to a specific cooperativity within the dinuclear unit. In spite of the incomplete character of the transition, the proportion of electronically dissymmetric species SQ is very small.

It would be quite unreasonable to generalize the results presented above to all of the polymetallic systems in which spin transition and exchange interaction coexist. Many investigations will be necessary before an overview can be obtained on this problem.

Registry No. **1**, 109584-92-1; **2**, 109584-93-2; **3**, 109612-95-5; $Fe(py)_4(NCS)_2$, 15154-78-6.

Supplementary Material Available: Listings of atomic parameters for hydrogen atoms (Table S1) and anisotropic thermal parameters for non-hydrogen atoms (Table S2) (2 pages); a table of calculated and observed structure factors (9 pages). Ordering information is given on any current masthead page.

(32) Real, J. A.; Borras, J.; Solans, X.; Font-Altaba, M. *Transition Met. Chem. (Weinheim, Ger.)*, in press.
(33) Real, J. A.; Borras, J.; Adler, P.; Gütlich, P., unpublished result.

Contribution from the Departments of Chemistry, Northwestern University, Evanston, Illinois 60208, and Oklahoma State University, Stillwater, Oklahoma 74078

Synthesis of Heterometallic Carbide Clusters Containing Three Iron Atoms: $[PPN]_2[MFe_3(CO)_{13}C]$ (M = Cr, W), $[PPN]_2[Cr_2Fe_3(CO)_{16}C]$, $Rh_2Fe_3(CO)_{14}C$, and $[PPN][Rh_3Fe_3(CO)_{15}C]$

Joseph A. Hriljac,[†] Elizabeth M. Holt,*[‡] and Duward F. Shriver*[†]

Received January 14, 1987

Redox-condensation reactions involving $[PPN]_2[Fe_3(CO)_9(CCO)]$ and electrophilic transition-metal reagents lead to $[PPN]_2[MFe_3(CO)_{13}C]$ (M = Cr, W), $[PPN]_2[Cr_2Fe_3(CO)_{16}C]$, $Rh_2Fe_3(CO)_{14}C$, and $[PPN][Rh_3Fe_3(CO)_{15}C]$. Variable-temperature ^{13}C NMR spectroscopy was employed to assign the structures of the tetranuclear clusters and $Rh_2Fe_3(CO)_{14}C$ in solution. An improved synthesis of $[PPN][RhFe_3(CO)_{12}C]$ and more complete variable-temperature (ca. −130 to +20 °C) ^{13}C NMR spectra of this cluster and $[PPN][MnFe_3(CO)_{13}C]$ are discussed. All of the tetranuclear clusters are assigned butterfly metal geometries with the heterometals located at hinge sites. Attempts to prepare iron–molybdenum carbide clusters are discussed. The structure of $[PPN][Rh_3Fe_3(CO)_{15}C]$ was determined by a single-crystal X-ray diffraction study and was found to consist of a trigonal-antiprismatic metal array with the carbide ligand within the metal polyhedron. The iron atoms define one of the trigonal faces and the rhodium atoms define the other. Crystal data for $[PPN][Rh_3Fe_3(CO)_{15}C]$: monoclinic, space group $P2_1/n$, a = 16.220 (6) Å, b = 9.282 (3) Å, c = 35.17 (3) Å, β = 94.84 (5)°, Z = 4.

Introduction

Transition-metal carbide clusters form a very interesting class of organometallic compounds. These clusters contain a carbon atom bonded only to metal atoms, and therefore their study plays a central role in defining the structural, bonding, and reactivity aspects of metal–carbon bonds. They may also be useful as models of the reactive carbide species that form on metal surfaces during CO hydrogenation reactions.[1,2]

The first report of reactivity at a carbide ligand was by Bradley and co-workers,[3] who demonstrated that the carbide ligand in a butterfly cluster with four metal atoms is subject to attack. This is in contrast to what had been found earlier for pentametallic clusters.[4,5] Studies of these butterfly cluster compounds by several research groups have demonstrated that reactions of the carbide ligands can lead to the formation of C–H and C–C bonds.[2,6]

Carbide reactivity is unique to the tetranuclear butterfly clusters. It was therefore of interest to study similar systems to try to understand the factors that relate to this reactivity and to try and extend the known reaction pathways. This work is directed toward the synthesis of new heterometallic carbide clusters, especially those that should contain reactive carbide ligands. The synthetic methodology that was chosen was to use the trimetallic cluster $[Fe_3(CO)_9(CCO)]^{2-}$ in redox-condensation reactions.[7] We previously demonstrated that this ketenylidene cluster is a useful carbide precursor.[8,9]

[†] Northwestern University.
[‡] Oklahoma State University.

(1) Tachikawa, M.; Muetterties, E. L. *Prog. Inorg. Chem.* **1981**, *28*, 203 and references therein.
(2) Bradley, J. S. *Adv. Organomet. Chem.* **1983**, *22*, 1 and references therein.
(3) Bradley, J. S.; Ansell, G. B.; Hill, E. W. *J. Am. Chem. Soc.* **1979**, *101*, 7417.
(4) Cooke, C. G.; Mays, M. J. *J. Organomet. Chem.* **1975**, *88*, 231.
(5) Kolis, J. W.; Basolo, F.; Shriver, D. F. *J. Am. Chem. Soc.* **1982**, *104*, 5626.
(6) Bogdan, P. L.; Woodcock, C.; Shriver, D. F. *Organometallics*, **1987**, *6*, 1377.
(7) Chini, P.; Heaton, B. T. *Top. Curr. Chem.* **1977**, *71*, 1.
(8) Kolis, J. W.; Holt, E. M.; Hriljac, J. A.; Shriver, D. F. *Organometallics* **1984**, *3*, 496.
(9) Hriljac, J. A.; Swepston, P. N.; Shriver, D. F. *Organometallics* **1985**, *4*, 158.

0020-1669/87/1326-2943$01.50/0